Journal of *Marine Science and Engineering*

MDPI

Article

Phylogenetic Position of the Morphologically Ambiguous Genus *Leiochrides* (Annelida: Capitellidae) Revealed by Its First Complete Mitogenome

Dae-Hun Kim [1,†], Junsang Youn [2,†], Junil Ko [2,†], Hyeryeong Oh [3], Haelim Kil [2], Seong-il Eyun [2,*] and Man-Ki Jeong [4,*]

[1] Department of Environmental Oceanography, Chonnam National University, Yeosu 59626, Republic of Korea
[2] Department of Life Science, Chung-Ang University, Seoul 06974, Republic of Korea
[3] Interdisciplinary Program of Bigdata Fishery Resources Management, Graduate School, Chonnam National University, Yeosu 59626, Republic of Korea
[4] Department of Smart Fisheries Resources Management, Chonnam National University, Yeosu 59626, Republic of Korea
* Correspondence: eyun@cau.ac.kr (S.-i.E.); jmgdeux@jnu.ac.kr (M.-K.J.)
† These authors contributed equally to this work.

Abstract

The family Capitellidae performs critical roles in bioturbation and sediment remediation within global marine benthic ecosystems. However, they are a taxonomically challenging group due to their simple morphology and a 'morphological mosaic', where traditional classificatory traits, such as thoracic chaetiger counts, appear convergently across genera. Previous multi-locus studies (using 18S, 28S, H3, and COI) first highlighted this conflict, revealing the polyphyly of major genera like *Notomastus* and even *Leiochrides* itself (based on unidentified specimens). More recently, mitogenomic studies uncovered massive gene order rearrangements and a conflicting topology but did not include *Leiochrides*. Critically, with no complete mitogenome reported for a formally identified *Leiochrides* species, its true phylogenetic position and the validity of its polyphyly remain unresolved. To address this critical gap, we sequenced and characterized the first complete mitochondrial genome from a formally identified species, *Leiochrides yokjidoensis*, recently described from Korean waters. The complete mitogenome was 17,933 bp in length and included the typical 13 protein-coding genes (PCGs), 2 ribosomal RNAs (rRNAs), and 22 transfer RNAs (tRNAs). Gene order (GO) analysis revealed the occurrence of gene rearrangements in Capitellidae and in its sister clade, Opheliidae. A phylogenomic analysis using the amino acid sequences of 13 PCGs from 30 species established the first robust systematic position for the genus *Leiochrides* (based on this formally identified species). Phylogenetic results recovered *Leiochrides* as a sister group to the clade comprising *Mediomastus*, *Barantolla*, *Heteromastus*, and *Notomastus hemipodus* (BS 99%). This distinct placement confirms that *Leiochrides* represents an independent evolutionary lineage, phylogenetically separate from the polyphyletic *Notomastus* complex, despite their morphological similarities. Furthermore, our analysis confirmed the polyphyly of *Notomastus*, with *N. hemipodus* clustering distinctly from other *Notomastus* species. Additionally, signatures of positive selection were detected in *ND4*, and *ND5* genes, suggesting potential adaptive evolution to the subtidal environment. This placement provides a critical, high-confidence anchor point for the genus *Leiochrides*. It provides a reliable reference to investigate the unresolved polyphyly suggested by previous multi-locus studies and provides compelling evidence for the hypothesis that thoracic chaetiger counts are of limited value for inferring phylogenetic relationships. This study provides the foundational genomic cornerstone for *Leiochrides*,

Academic Editor: Nguyen Hong Nguyen

Received: 10 December 2025
Revised: 11 January 2026
Accepted: 12 January 2026
Published: 15 January 2026

representing an essential first step toward resolving the systematics of this taxonomically challenging family.

Keywords: Sedentaria; phylogenomics; systematics; gene rearrangement; positive selection; polyphyly; *Notomastus*

1. Introduction

Annelida, a diverse phylum of segmented worms, constitutes a critical component of global marine biodiversity and ecological functioning, particularly within soft-bottom benthic ecosystems [1]. The family Capitellidae Grube, 1862 [2], has a complex systematic history; it was once grouped with Clitellata due to similarities in external and internal (pharyngeal) morphology, followed by a long association with other sedentary polychaetes. The family currently comprises 42 genera and 224 recognized species [3] and is ecologically renowned. As key subsurface deposit-feeders, they ingest buried sediment particles, playing a foundational role in nutrient cycling [4]. Their continuous burrowing and ventilation activities (bioirrigation) are fundamental to benthic biogeochemical cycling, as they transport oxygen into anoxic sediment layers, stimulate microbial decomposition, and thus facilitate the remediation of organically enriched or polluted sediments [5,6]. Consequently, many capitellid species are recognized as opportunistic indicators, often dominating marine sediments following major disturbance events [7].

Despite this ecological ubiquity, Capitellidae remains one of the most taxonomically challenging groups in Polychaeta [7,8]. The family's classification is notoriously fragmented; the fact that nearly half of its 42 described genera (approx. 24) are considered monospecific (containing only a single species) highlights the historical difficulty in establishing robust generic definitions [3,9]. This chaos stems from their "notoriously" simple body plan, which lacks complex appendages (like palps or elaborate parapodia) and exhibits a uniform, thread-like appearance [9–11]. Traditionally, generic-level classification has relied heavily on a limited suite of morphological characters: primarily the number of thoracic chaetigers and the distribution patterns of chaetae (i.e., capillaries vs. hooded hooks) [7,9–11].

This reliance on a limited set of characters has created a significant 'morphological mosaic', leading to profound taxonomic ambiguity. The systematic placement of the genus *Leiochrides* Augener, 1914 [12], exemplifies this challenge. *Leiochrides* is defined by possessing 12 thoracic chaetigers [9,13]. This count numerically separates it from numerous key genera such as *Notomastus* (11 chaetigers), *Heteromastus* (11 chaetigers), and *Decamastus* (10 chaetigers), as well as from *Dasybranchus* (13 chaetigers) and *Leiocapitella* (14 chaetigers) [9,13–16].

However, the phylogenetic value of this segment count is highly questionable, as the chaetal arrangement patterns appear to be homoplastic across these numerical boundaries. The generic diagnosis of *Leiochrides* itself has a convoluted history, reflecting this ambiguity. While historically defined by having all capillary chaetae [9,13], this definition was challenged by Hartman [17,18], who argued for the inclusion of species with "transitional" segments (e.g., presence of notopodial capillaries and neuropodial hooded hooks in the same segment) on the posterior-most chaetigers. This expanded definition [19,20] gained wide acceptance, particularly after the synonymization of *Pseudomastus* Capaccioni-Azzati & Martin, 1992 [21] (which was defined by this transitional trait) under *Leiochrides* by Jeong et al. [13]. This taxonomic decision confirmed that this trait is likely an intraspecific or intrageneric variation, not a genus-level diagnostic feature [13]. This exact 'transitional' pattern also appears convergently across multiple genera with different thoracic counts:

for instance, *Not omastus* (11 chaetigers) includes species such as *N. sunae* and *N. angelicae*, which are characterized by possessing neuropodial hooded hooks on the last thoracic segment (TC11) [22,23]. *Decamastus* (10 chaetigers), such as in the type species *D. gracilis*, possesses hooks in the neuropodia of the last one or two thoracic segments (TC9–10) [20,24]; and *Leiocapitella* (12–17 chaetigers) is likewise diagnosed by a transitional final thoracic segment [9,25,26]. Furthermore, the genus *Scyphoproctus*—defined by its unique anal funnel, not its thorax [20]—exhibits extreme ambiguity. Its thoracic segment count is highly variable (reported as 9–14 chaetigers), and it contains species such as *S. oculatus* (mirroring the 'all capillary' *Leiochrides* pattern) as well as species like *S. lumenalis* (possessing the 'transitional' pattern) [19,27]. This morphological mosaic, where key chaetal patterns (e.g., 'transitional segments') converge across genera with 9–17 chaetigers, makes it impossible to validate these genera or infer their relationships based on morphology alone.

Previous molecular-phylogenetic studies initiated the effort to resolve this conflict between morphological definitions and evolutionary lineages. A foundational study by Tomioka et al. [8], focusing on Japanese taxa including key problematic genera like *Notomastus* and *Heteromastus*, provided the first major test of the traditional classification using concatenated data of four nuclear and mitochondrial gene fragments (18S rDNA, 28S rDNA, H3, and COI). While this study successfully confirmed the monophyly of Capitellidae (in contrast to [1]), its findings provided the first direct molecular evidence of the failure of the classical system. It demonstrated that traditional diagnostic characters—specifically, "head type; number of thoracic segments; number of segments with capillary chaetae"—were "not informative" for delineating natural groups. This was exemplified by their key finding that the genera *Notomastus* and *Barantolla* were not monophyletic, instead forming a mixed, well-supported clade. This result strongly suggests that the true phylogenetic relationships are more complex than the traditional generic definitions allow. Although this study was pivotal in establishing this problem awareness, most other nodes in their analysis remained weakly supported, highlighting that the limited number of genetic loci (4 partial genes) provided insufficient phylogenetic signal to fully resolve the family's backbone.

More recently, the first mitogenomic study of the family by Su et al. [28] revealed even deeper complexities. This study, using 13 PCGs (and a larger concatenated dataset including nuclear 18S, 28S, and H3 genes) from 8 species, uncovered massive gene order (GO) rearrangements within the family, challenging the long-held view of conserved annelid mitogenomes. Their analysis proposed a new framework, splitting the family (excluding *Capitella*) into a "Conserved Group" (*Mediomastus*, *Barantolla*) and a "Rearranged Group" (*Notomastus*, *Notodasus*), with the latter even possessing a rare Group II intron. Critically, this new mitogenome-dominated phylogenomic topology revealed a significant conflict with the nuclear-dominated multi-locus topology of Tomioka et al. [8]. Specifically, the former (driven by 13 mitochondrial PCGs + 3 partial nuclear genes) recovered the *Mediomastus* group (Clade 1) as the basal lineage, whereas the latter topology (driven by 3 partial nuclear genes + 1 partial mitochondrial gene) had recovered *Capitella* (Clade B) as basal. This discordance, resulting from the different genomic data types and their respective weightings, suggests that the family's evolution is fraught with complex genomic histories and potential analytical artifacts (like Long Branch Attraction).

This leads to the critical gap addressed by our study. While these pivotal molecular studies [8,28] did include genetic data from *Leiochrides*, the data itself was the source of ambiguity. Both datasets relied on three unidentified *Leiochrides* specimens (sp. 1 (Hiroshima, Japan), sp. 2 (Kanagawa, Japan), sp. 3 (Okinawa, Japan)), which were shown to be polyphyletic. Consequently, although the polyphyletic placement was confirmed, the systematic implications remained unresolved. Furthermore, publicly available mitochondrial DNA information for this genus remains limited to a single partial 529 bp COI sequence

from another unverified *Leiochrides* sp1. To date, no complete mitochondrial genome has been reported for *Leiochrides* based on a formally identified species.

This significant data gap prevents a comprehensive understanding of genome evolution within the family. Therefore, this study presents the first complete mitochondrial genome for a formally identified species of the genus *Leiochrides*, using the recently described Korean species *Leiochrides yokjidoensis* Jeong, Wi & Suh, 2017 [13]. The primary aim of this study is to (1) characterize its complete genomic structure, gene content, and organization, and (2) utilize this new genomic data to conduct a robust phylogenomic analysis across 7 families to establish the systematic position of *Leiochrides* within the recently proposed mitogenomic framework; and (3) examine signatures of positive selection to elucidate the adaptive evolution of this species. This placement provides a critical, high-confidence anchor point for the genus, allowing for a re-evaluation of the polyphyly hinted at by previous studies. Although a definitive test of generic monophyly requires sequencing additional *Leiochrides* species, this study provides the foundational genomic cornerstone for the genus. It represents a critical first step, providing a reliable reference point to which future phylogenomic investigations into this taxonomically challenging family can be compared.

2. Materials and Methods

2.1. Sample Collection and Processing

Leiochrides yokjidoensis specimens were obtained from subtidal zones (26–60 m depth) across the southern coast of Korea, including Geomundo Island, Busan, and the outer main channel of Gwangyang Bay, from March 2024 to May 2025 (Type Locality: Yokjido Island) (Figure 1). Samples were obtained using a Smith–McIntyre grab sampler. The collected sediments were sieved through a 0.5 mm mesh, and specimens were sorted live on board. Specimens were relaxed using a 7.5% $MgCl_2$ solution to prevent contraction. For morphological examination, samples were fixed in 10% neutral buffered formalin and subsequently transferred to 80% ethanol. Specimens were examined and photographed with a Stemi 305 stereomicroscope (ZEISS, Oberkochen, Germany) and an Eclipse Ci-L compound microscope (Nikon, Tokyo, Japan), both equipped with digital cameras. Two staining methods were employed to visualize different morphological features. To observe the species-specific patterns of glandular tissues, specimens were stained with a methyl green solution. Specimens were briefly immersed in the staining solution (approx. 60 s) until a distinct color pattern emerged, then rinsed in 80% ethanol for differentiation. Separately, Shirlastain A solution (SDLATLAS, Rock Hill, SC, USA) was used to enhance the overall contrast of morphological structures and facilitate observation. Specimens were immersed for a short period (approx. 30 s) and subsequently rinsed. Staining results from both methods were documented through photography.

2.2. Species Identification Criteria

The specimen used for genomic sequencing was unequivocally identified as *Leiochrides yokjidoensis* Jeong, Wi & Suh, 2017 [13], based on the combination of the following key diagnostic characters, which distinguish it from other congeners (Figure 2):

1. Chaetal Formula: Thoracic chaetigers 1–11 bear only capillary chaetae in both noto- and neuropodia. The final thoracic segment, TC12, is a transitional segment bearing capillary chaetae in the notopodium and hooded hooks in the neuropodium.
2. Chaetiger 1: The first thoracic chaetiger (TC1) is uniramous, possessing only notopodial capillary chaetae (neuropodia are absent).

3. Hook Dentition: Abdominal hooded hooks, examined under high magnification (1000×) with the compound microscope, showed a main fang surmounted by 8–10 small apical teeth.
4. Branchiae: Branchiae present on posterior abdominal segments as 2–4 digitate filaments near notopodia. There are approximately ten preanal chaetigers without branchiae.
5. MGSP: The staining pattern was consistent with the type description of *L. yokjidoensis*, showing strong staining on TC6–9 and distinct patterns on posterior segments.

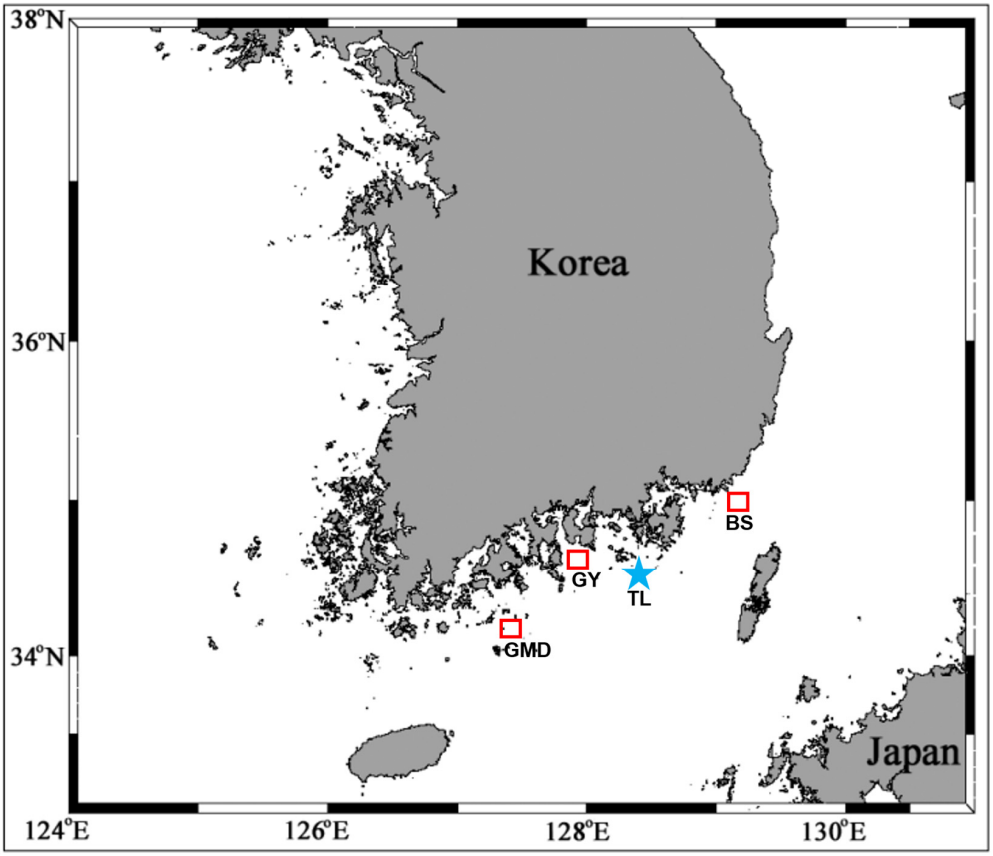

Figure 1. Map showing sampling stations along the southern coast of Korea. The red box indicates the location(s) in the subtidal zone (26–60 m depth) where specimens of *Leiochrides yokjidoensis* were collected. Abbreviations: GMD, Geomundo Island station; GY, Gwangyang station; BS, Busan station; TL, Type locality of *Leiochrides yokjidoensis*.

A posterior portion of the specimen was subsampled for molecular analysis, while the anterior portion, including the thorax, was retained as a voucher specimen. All examined specimens, including newly collected material, are deposited at Chonnam National University Specimen Collection, South Korea (JUMA_20251211_001, JUMA_20250901_007, JUMA_20260106_001).

2.3. Mitogenome Sequencing and Reconstruction

Total genomic DNA was extracted using the QIAGEN Blood and Cell Culture DNA Mini Kit (QIAGEN, Hilden, Germany) according to the manufacturer's instructions. A paired-end library (151 bp) was constructed using the TruSeq DNA Nano 550 Kit (Illumina, Inc., San Diego, CA, USA), and sequencing was performed on an Illumina Novaseq X Plus platform by JS Link Inc. (Seoul, Republic of Korea) (Table 1).

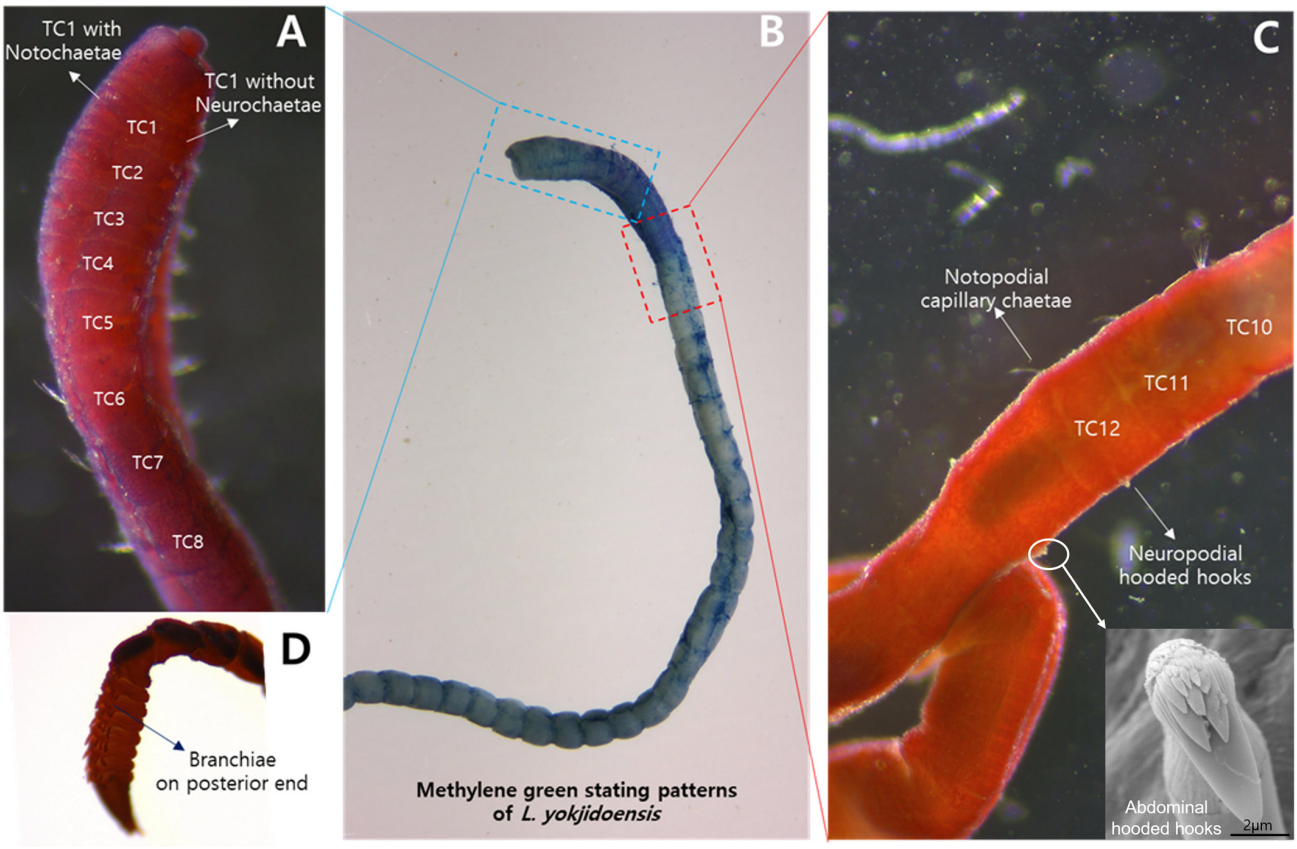

Figure 2. Key diagnostic features of *Leiochrides yokjidoensis*. (**A**) Anterior end (lateral view), showing uniramous first chaetiger. (**B**) Methyl Green Staining Pattern (MGSP) of the anterior region. (**C**) Thoracic-abdominal junction (lateral view), showing the transitional segment (chaetiger 12) with neuropodial hooks. (**D**) Branchiae of posterior end of examined specimen.

Table 1. Summary of statistics for next-generation sequencing data and the mitochondrial genome assembly workflow.

	Leiochrides yokjidoensis	
Sequencing	Sequencing System Library Construction Sequencing layout (bp) Fragment size (bp)	Illumina Novaseq X Plus TruSeq DNA Nano 151 × 2 550
Raw Data	Raw reads Raw bases (bp) Q30 (%)	115,488,548 17,438,770,748 94.90
Filtered Data	Clean reads Clean bases (bp) Total length (bp)	115,488,548 16,697,248,234 17,933
Mitochondrial genome assembly	GC content (%) Number of protein-coding genes	45.08 13

Before assembly, raw reads were processed with Trim_Galore (ver. 0.6.10) [29] to eliminate adapters and low-quality bases (Phred score < 30). The de novo assembly of the *Leiochrides yokjidoensis* mitogenome was carried out using MitoZ (ver. 3.6) [30] based on the clean reads. Subsequent gene annotation was performed using MITOS2 (ver. 2.1.9) [31] and ARWEN (ver. 1.2.3) [32]. Finally, the circular map of the assembled genome was generated using Circos (ver. 0.69-8) [33–35].

2.4. Phylogenomic Reconstruction

To investigate phylogenetic relationships within the subclass Sedentaria, we performed a phylogenomic analysis based on the amino acid sequences of 13 mitochondrial protein-coding genes (PCGs). The dataset comprised 30 species, including *Leiochrides yokjidoensis*, with two species from the subclass Errantia used as outgroups. Publicly available mitogenome sequences were retrieved from the NCBI database; for entries lacking annotation, the 13 PCGs were identified using MitoZ (ver. 3.6) [30] and MITOS2 (ver. 2.1.9) [31]. Sequence alignment for each PCG was conducted using MAFFT (ver. 7.525) [36] and PAL2NAL (ver. 14.1) [37].

To reduce the potential effects of long-branch attraction, only the first and second codon positions of the 13 PCGs were retained for subsequent phylogenetic analyses. Optimal evolutionary models were selected based on the Bayesian Information Criterion (BIC) using PartitionFinder2 (ver. 2.1.1) [38]. The dataset was partitioned into three subsets, and the GTR + I + G model (General Time-Reversible model with Invariant sites and Gamma-distributed rate variation) was selected as the best-fit model for all subsets. Phylogenetic reconstruction was performed using Maximum Likelihood (ML) and Bayesian Inference (BI) approaches. The ML analysis was executed in RAxML-NG (ver. 1.2.2) [39] with 1000 bootstrap replicates to evaluate nodal support. BI analysis was conducted using MrBayes (ver. 3.2.7) [40]. We ran two independent Markov Chain Monte Carlo (MCMC) chains for 1×10^7 generations, sampling every 1000 generations with a chain temperature of 0.02. Convergence was confirmed when the average standard deviation of split frequencies dropped below 0.01. After discarding the first 25% of trees as burn-in, a majority-rule consensus tree was computed. The final tree topologies were visualized using FigTree (ver. 1.4.4) [41].

2.5. Tests for Positive Selection

To detect genomic signatures of adaptive evolution in response to environmental pressures, we identified positively selected genes (PSGs) among the mitochondrial PCGs using the CodeML program in PAML [42]. The input topology was the unrooted ML tree derived from the 13 PCGs with branch lengths removed. Nucleotide sequences were codon-aligned using PAL2NAL (ver. 14.1) [37]. We applied both the site model and the branch-site model for selection analysis. We analyzed site-specific selection using site models (model = 0, NSsites = 0 1 2 3 7 8, fix_omega = 0). We then performed the branch-site test by comparing a null model (model = 2, NSsites = 2, fix_omega = 1) against an alternative model (model = 2, NSsites = 2, fix_omega = 0). The site model allows the nonsynonymous-to-synonymous substitution ratio (ω = dN/dS) to vary across codon sites, whereas the branch-site model allows ω to diverge in the foreground branch relative to the background branches. Statistical significance was assessed using Likelihood Ratio Tests (LRTs) approximating a chi-square (χ^2) distribution. Sites were considered to be under positive selection if the LRT was significant ($p < 0.05$) and the calculated ω exceeded 1.

3. Results and Discussion

3.1. General Features of the Mitochondrial Genome

We successfully assembled the complete circular mitogenome of *Leiochrides yokjidoensis* (17,933 bp; GenBank Accession No. PX614612) using high-quality sequencing data. The assembly was based on 115,488,548 paired-end reads generated via the Illumina platform, from which 16.7 Gb of clean bases were retained (Q30 $\geq$ 94.90%) after rigorous filtering (Table 1).

The genome architecture comprises the typical metazoan set of 37 genes—13 protein-coding genes (PCGs), 2 ribosomal RNAs (12S and 16S), and 22 transfer RNAs—all of which

are encoded on the heavy strand (H-strand) (Table 2 and Figure 3). Coding regions account for 81.10% of the entire genome, with PCGs alone constituting 61.50%.

Table 2. Gene organization and annotated features of the *Leiochrides yokjidoensis* mitochondrial genome.

Gene	Position	Length (bp)	Initiation Codon	Stop Codon	Anti-Codon	Strand
tRNA-Trp (trnW)	617–680	65			TCA	+
NADH dehydrogenase subunit 3 (ND3)	685–1032	349	ATG	TAG		+
NADH dehydrogenase subunit 4L (ND4L)	1041–1335	295	ATG	TAG		+
tRNA-Tyr (trnY)	1336–1400	66			GTA	+
ATP synthase F0 subunit 6 (ATP6)	1401–2045	645	ATG	TAA		+
tRNA-Ser (trnS)	2105–2171	68			TGA	+
tRNA-Val (trnV)	2171–2235	66			TAC	+
tRNA-Thr (trnT)	2236–2298	64			TGT	+
NADH dehydrogenase subunit 2 (ND2)	2303–3265	963	ATG	TAA		+
Cytochrome c oxidase subunit III (COX3)	3302–4093	792	GTG	TAG		+
tRNA-Leu (trnL)	4208–4269	63			TAG	+
NADH dehydrogenase subunit 1 (ND1)	4270–5208	940	GTG	TAA		+
NADH dehydrogenase subunit 6 (ND6)	5209–5691	484	ATG	TAA		+
Cytochrome b (COB)	5765–6874	1111	ATG	TAA		+
NADH dehydrogenase subunit 5 (ND5)	8547–10,277	1732	GTG	TAA		+
NADH dehydrogenase subunit 4 (ND4)	10280–11,572	1294	ATG	TAG		+
tRNA-Asn (trnN)	11,574–11,636	64			GTT	+
tRNA-Met (trnM)	11,637–11,700	65			CAT	+
tRNA-His (trnH)	11,733–11,794	63			GTG	+
tRNA-Leu (trnL)	11,794–11,856	64			TAA	+
tRNA-Ile (trnI)	11,858–11,921	65			GAT	+
tRNA-Arg (trnR)	11,923–11,986	65			TCG	+
tRNA-Phe (trnF)	11,987–12,051	66			GAA	+
tRNA-Glu (trnE)	12,284–12,348	66			TCC	+
12S ribosomal RNA (s-rRNA)	12,349–13,186	839				+
tRNA-Gln (trnQ)	13,184–13,251	69			TGG	+
16S ribosomal RNA (l-rRNA)	13,250–14,494	1246				+
tRNA-Ala (trnA)	14,470–14,533	65			TGV	+
tRNA-Asp (trnD)	14,535–14,598	65			GTC	+
ATP synthase F0 subunit 8 (ATP8)	14,599–14,760	163	ATG	TAA		+
tRNA-Pro (trnP)	15,017–15,081	66			TGG	+
tRNA-Lys (trnK)	15,927–15,994	69			TTT	+
tRNA-Ser (trnS)	16,013–16,077	65			TCT	
tRNA-Cys (trnC)	16,104–16,168	66			GCA	+
tRNA-Gly (trnG)	16,171–16,235	66			TCC	+
Cytochrome c oxidase subunit II (COX2)	16,236–16,946	712	ATG	TAG		+
Cytochrome c oxidase subunit I (COX1)	17,004-618	1548	ATA	TAG		+

In terms of nucleotide composition, the genome exhibits a distinct A + T bias (54.92% overall), with base proportions of 19.15% A, 35.77% T, 27.89% G, and 17.19% C. Analysis of the 13 PCGs revealed that while the canonical ATG start codon is used in nine genes, *COX3*, *ND1*, and *ND5* utilize GTG, and *COX1* initiates with ATA. Termination codons consist of either TAA (eight genes) or TAG (five genes) (Table 2).

3.2. Phylogeny and Synteny

To overcome the limitations of morphological identification—specifically the scarcity of type specimens and ambiguous original descriptions—we employed a phylogenomic approach to resolve the systematic position of *Leiochrides yokjidoensis*. While morphology alone often yields uncertain taxonomic results, genomic data provide a robust framework for addressing these complexities. We constructed a Maximum Likelihood (ML) tree based on the amino acid sequences of 13 mitochondrial protein-coding genes (PCGs) from

26 representative species of the subclass Sedentaria (Table 3). This multi-locus dataset offers significantly higher resolution for phylogenetic inference than single-gene markers [43,44].

Table 3. List of the 26 mitochondrial genomes utilized in this phylogenomic analysis, including taxonomic details and GenBank accession numbers.

Family	Genus	Species	Accession Number	Type Locality	Sampling Locality	Reference
Capitellidae	*Leiochrides*	*Leiochrides yokjidoensis*	PX614612	Yokjido, Korea	Geomundo, Korea	This study
	Notomastus	*Notomastus* sp.	LC661358.1	-	Wakayama, Japan	Kobayashi et al. [45]
		Notomastus sp. A	PP133661.1	-	Hong Kong, China	Su et al. [28]
		Notomastus sp. B	PQ010758.1	-	Hainan, China	Su et al. [28]
		Notomastus hemipodus	PV742383.1	North Carolina, USA	Vancouver, Canada	Acharya-Patel et al. [46]
	Notodasus	*Notodasus* sp. A	PP133663.1	-	Hong Kong, China	Su et al. [28]
		Notodasus sp. B	PQ010757.1	-	Hainan, China	Su et al. [28]
		Notodasus sp. C	PP133662.1	-	Fujian, China	Su et al. [28]
	Capitella	*Capitella teleta*	PP133665.1	Massachusetts, USA	Shandong, China	Su et al. [28]
		Capitella capitata	PV742352.1	Greenland	Vancouver, Canada	Acharya-Patel et al. [46]
	Heteromastus	*Heteromastus filobranchus*	PV742385.1	Vancouver, Canada	Canada	Acharya-Patel et al. [46]
	Mediomastus	*Mediomastus* sp.	PP133664.1	-	Guangdong, China	Su et al. [28]
	Barantolla	*Barantolla* sp.	PQ010756.1	-	Hainan, China	Su et al. [28]
Arenicolidae	*Abarenicola*	*Abarenicola claparedi*	LC707921.1	Mediterranean Sea	Hokkaido, Japan	Kobayashi et al. [47]
Maldanidae	*Asychis*	*Asychis amphiglyptus*	NC_069297.1	South Georgia, UK	-	-
	Clymenella	*Clymenella koellikeri*	PQ593498.1	Fiji, EEZ	-	-
		Clymenella torquata	NC_006321.1	New Jersey, USA	Massachusetts, USA	Jennings and Halanych [48]
	Euclymene	*Euclymene annandalei*	OM273170.1	India	-	-
	Lumbriclymenella	*Lumbriclymenella robusta*	OP537514.1	South Georgia, UK	-	-
	Maldane	*Maldane sarsi*	OP694172.1	Sweden	-	-
	Metasychis	*Metasychis gotoi*	OP605751.1	Japan, EEZ	-	-
	Nicomache	*Nicomache* sp.	PQ593499.1	-	-	-
	Petaloproctus	*Petaloproctus* sp.	PQ593501.1	-	-	-
	Praxillella	*Praxillella affinis*	PQ593500.1	Norway, EEZ	-	-
	Sabaco	*Sabaco sinicus*	PQ741859.1	China	-	-
Cossuridae	*Cossura*	*Cossura aciculata*	PV151471.1	China	China	-
Opheliidae	*Armandia*	*Armandia* sp.	LC661359.1	-	Wakayama, Japan	Kobayashi et al. [45]
Orbiniidae	*Orbinia*	*Orbinia latreillii*	NC_007933.1	La Rochelle, France	Bretagne, France	Bleidorn et al. [49]
Phyllodocidae	*Phyllodoce*	*Phyllodoce medipapillata*	NC_087881.1	USA	California, USA	Huč et al. [50]
		Phyllodoce koreana	PQ510072.1	Korea	Korea	Kim et al. [51]

The resulting phylogeny strongly supported the monophyly of the family Capitellidae (BS = 100%, PP = 1.00). Within this clade, *L. yokjidoensis* was recovered as the sister group to the clade comprising *Mediomastus*, *Barantolla*, *Heteromastus*, and *Notomastus hemipodus* (BS = 99%), a placement that diverges from traditional morphological classifications. Additionally, Capitellidae formed a robust sister-group relationship with Opheliidae (BS = 99%), suggesting a shared evolutionary history. This affinity is further reinforced by the distinct patterns of mitochondrial gene rearrangement observed in both families (Figure 4).

To complement these phylogenetic findings, we performed a comparative analysis of mitochondrial gene synteny across the 30 polychaete species (Figure 4, right). Our analysis revealed a striking correlation between phylogenetic branch lengths (evolutionary rate) and genomic structural stability. While the outgroup and most other sedentarian families exhibited a conserved ancestral gene arrangement, Capitellidae showed three distinct evolutionary modes correlated with their substitution rates:

1. Conserved Group (Short Branches): The clade comprising *Mediomastus*, *Barantolla*, *Heteromastus*, and *Notomastus hemipodus* exhibited relatively short branch lengths,

indicating a slower rate of molecular evolution. Correspondingly, these species shared an identical and conserved gene order, suggesting high genomic stability in this lineage.

2. Hyper-variable Group (Intermediate/Long Branches): The "Rearranged Group" (*Notomastus* sp., *Notomastus* sp. A, *Notomastus* sp. B, *Notodasus* sp. A, *Notodasus* sp. B and *Notodasus* sp. C) displayed longer branch lengths. Remarkably, all four examined *Notomastus* species (*N. hemipodus*, *Notomastus* sp., *Notomastus* sp. A, and *Notomastus* sp. B) exhibited different gene arrangements from each other. This extreme variability within a single nominal genus, coupled with their polyphyletic placement, indicates a "hotspot" of genomic instability and further supports the need for taxonomic revision of *Notomastus*.
3. Divergent Group (Longest Branches): The distinct lineages of *Leiochrides yokjidoensis* and the genus *Capitella* exhibited the longest branch lengths in the tree, indicative of rapid accelerated evolution. Consistent with this high substitution rate, both genera exhibit unique and heavily rearranged mitochondrial gene orders relative to other groups; the two *Capitella* species share the same mitochondrial gene order, while *Leiochrides* differs markedly from *Capitella*, consistent with their distant phylogenetic positions.

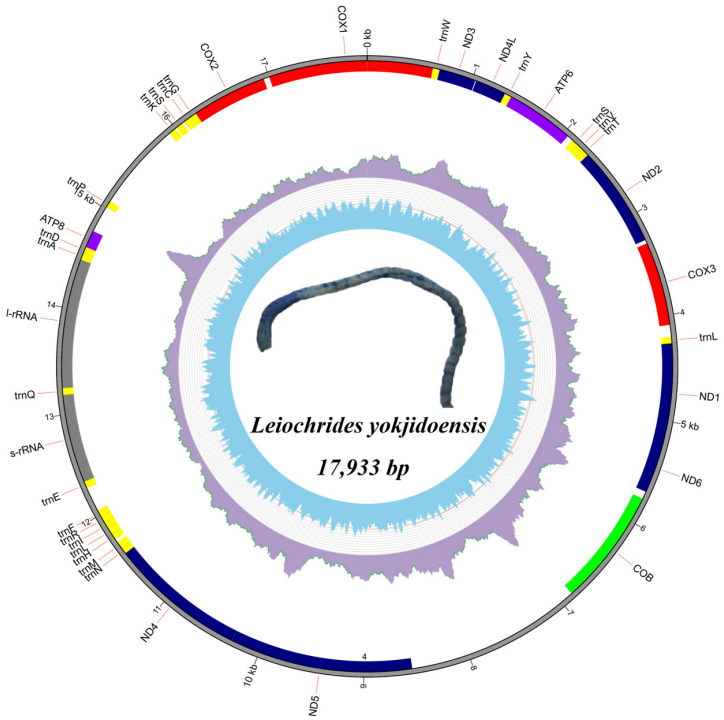

Figure 3. Map of the *Leiochrides yokjidoensis* mitochondrial genome. The innermost and middle rings display GC content (blue) and sequencing depth (purple), respectively. The outermost ring depicts protein-coding genes colored by family: *COX* (red), ATP synthase (purple), *COB* (green), and *ND* (navy). rRNAs and tRNAs are shown in gray and yellow.

Although limited by the current taxon sampling, these observations suggest a potential link within Capitellidae where lineages undergoing rapid sequence evolution (long branches) are also prone to extensive structural rearrangements. The unique gene order and rapid evolutionary rate of *Leiochrides* further highlight its distinct evolutionary trajectory, distinguishing it from the polyphyletic *Notomastus* complex and other related genera, despite their morphological resemblances.

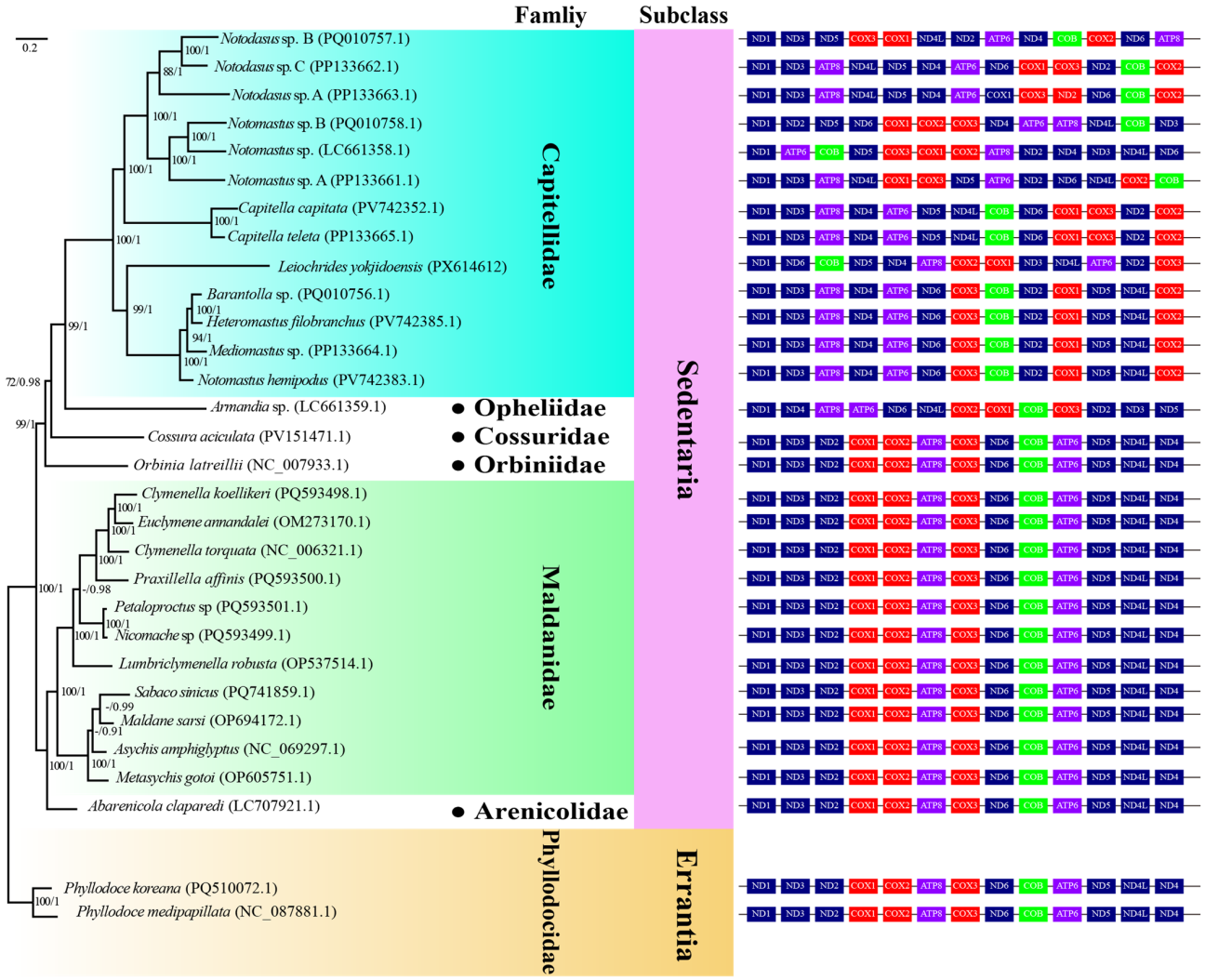

Figure 4. Phylogenetic reconstruction rooted with two outgroup species from the family Phyllodocidae. Nodal support values are displayed for Maximum Likelihood (ML) and Bayesian Inference (BI) analyses where support exceeds 70% (ML/BI). The color-coded blocks on the right indicate family-level classification. The scale bar denotes the relative rate of substitution per site. The genomic synteny of the 13 mitochondrial protein-coding genes (PCGs) is illustrated alongside the tree, with the arrangement standardized to begin with the ND1 gene.

3.3. Positive Selection Analysis

Although mitochondrial protein-coding genes (PCGs) are primarily constrained by purifying selection to maintain the functional integrity of oxidative phosphorylation, they can also exhibit signatures of adaptive evolution. To investigate these potential environmental adaptations, we evaluated selective pressures by calculating the ratio of non-synonymous to synonymous substitution rates (ω = dN/dS) across all 13 PCGs (Tables 4 and 5). The Site model analysis generally indicated purifying selection across the phylogeny. Although the likelihood ratio test comparing models M7 and M8 initially detected signals in both *ND4L* and *ND5* (Table 4), examination of parameter estimates revealed an ω value of 1 for *ND4L* (Table 6) [52]. Therefore, *ND4L* was under neutral evolution rather than positive selection. More importantly, the Branch-site model test, which focused specifically on the lineage leading to *Leiochrides yokjidoensis*, revealed stronger and statistically significant signatures of positive selection in three genes: *ND4*, *ND5*, and *ND6* (Table 5). However, *ND6* was excluded from the final candidates because the estimated proportion of sites under positive selection was zero ($p_2 = 0$) suggesting the absence of true adaptive signals. Specific amino

acid sites under positive selection were identified via Bayes Empirical Bayes (BEB) analysis (Tables 6 and 7). These results suggest that, while the mitochondrial genome is largely conserved, specific genes in *L. yokjidoensis* have undergone adaptive evolution, potentially facilitating metabolic adjustments to its subtidal benthic environment (26–60 m depth).

Table 4. Statistical outcomes of the positive selection analysis based on site models. Abbreviations: np, number of parameters; LRT, likelihood ratio test statistic.

Gene	M0 (37)	M1a (38)	M2a (40)	M3 (41)	M7 (38)	M8 (40)	Model Comparison (np)	LRTs
ATP6	−18,216.17475	−18,086.11357	−18,086.11357	−17,551.54513	−17,530.66051	−17,530.66246	M0 vs. M3 (4) M1a vs. M2a (2) M7 vs. M8 (2)	1329.2592 0 0.003888
ATP8	−4915.891856	−4815.027421	−4814.851827	−4713.267295	−4709.704374	−4709.70452	M0 vs. M3 (4) M1a vs. M2a (2) M7 vs. M8 (2)	405.24912 0.351188 0.000292
COX1	−26,830.58115	−26,700.24829	−26,700.24829	−25,753.3935	−25,737.72334	−25,736.49474	M0 vs. M3 (4) M1a vs. M2a (2) M7 vs. M8 (2)	2154.3753 0 2.457196
COX2	−14,386.37689	−14,344.30227	−14,344.30227	−13,834.47394	−13,833.0083	−13,833.00895	M0 vs. M3 (4) M1a vs. M2a (2) M7 vs. M8 (2)	1103.8059 0 0.001298
COX3	−14,686.20445	−14,564.92926	−14,564.92931	−14,027.43752	−14,010.6313	−14,010.63354	M0 vs. M3 (4) M1a vs. M2a (2) M7 vs. M8 (2)	1317.5339 0.000104 0.004478
COB	−23,974.19042	−23,798.6266	−23,798.6266	−22,897.66727	−22,864.7537	−22,864.75552	M0 vs. M3 (4) M1a vs. M2a (2) M7 vs. M8 (2)	2153.0463 0 0.003644
ND1	−21,684.92572	−21,371.14525	−21,371.14525	−20,589.39337	−20,552.08262	−20,552.02358	M0 vs. M3 (4) M1a vs. M2a (2) M7 vs. M8 (2)	2191.0647 0 0.11807
ND2	−28,666.00705	−28,409.10097	−28,409.10097	−27,794.59458	−27,760.01575	−27,760.0163	M0 vs. M3 (4) M1a vs. M2a (2) M7 vs. M8 (2)	1742.8249 0 0.001096
ND3	−8783.448956	−8603.506367	−8603.506367	−8284.0882	−8287.373649	−8287.374643	M0 vs. M3 (4) M1a vs. M2a (2) M7 vs. M8 (2)	998.72151 0 0.001988
ND4	−34,592.0451	−34,232.74772	−34,232.74772	−33,072.81786	−33,028.81993	−33,028.79363	M0 vs. M3 (4) M1a vs. M2a (2) M7 vs. M8 (2)	3038.4545 0 0.05259
ND4L	−8178.441719	−8140.187983	−8140.187983	−7922.090965	−7912.282848	−7908.560915	M0 vs. M3 (4) M1a vs. M2a (2) M7 vs. M8 (2)	512.70151 0 7.443866
ND5	−44,566.23379	−44,023.18734	−44,023.18734	−42,438.75504	−42,334.82236	−42,332.05566	M0 vs. M3 (4) M1a vs. M2a (2) M7 vs. M8 (2)	4254.9575 0 5.533394
ND6	−13,442.30588	−13,262.91993	−13,262.91993	−12,929.87655	−12,907.36782	−12,907.07133	M0 vs. M3 (4) M1a vs. M2a (2) M7 vs. M8 (2)	1024.8587 0 0.592974

Note. The critical values are $\chi^2_{2.5\%} = 5.99$ (i.e., 2 degrees of freedom at 5% significance), $\chi^2_{2.1\%} = 9.21$ (i.e., 2 degrees of freedom at 1% significance), $\chi^2_{4.5\%} = 9.48$ (i.e., 4 degrees of freedom at 5% significance), and $\chi^2_{4.1\%} = 13.27$ (i.e., 4 degrees of freedom at 1% significance). The LRT statistic, $2\Delta\ell$, is reported for all model comparisons.

Table 5. Statistical outcomes of the positive selection analysis based on the branch-site model. Abbreviations: np, number of parameters; LRT, likelihood ratio test statistic.

Gene Name	Null Model (np)	Alternative Model (np)	LRTs (*p*-Value)	Site Class	0	1	2a	2b
ATP6	−17,913.70553 (64)	−17,912.76472 (65)	1.881618 (0.17)	Proportion	0.51033	0.20768	0.20043	0.08156
				Background ω	0.09429	1	0.09429	1
				Foreground ω	0.09429	1	45.4215	45.4215
ATP8	−4672.201808 (64)	−4672.201805 (65)	0.000006 (0.998)	Proportion	0.21817	0.78183	0	0
				Background ω	0.086	1	0.086	1
				Foreground ω	0.086	1	1	1
COX1	−26,375.29311 (64)	−26,375.29226 (65)	0.0017 (0.967)	Proportion	0.8193	0.022	0.15455	0.00415
				Background ω	0.01875	1	0.01875	1
				Foreground ω	0.01875	1	1.01768	1.01768

Table 5. *Cont.*

Gene Name	Null Model (np)	Alternative Model (np)	LRTs (*p*-Value)	Site Class	0	1	2a	2b
COX2	−14,280.19673 (64)	−14,280.19673 (65)	0(1)	Proportion Background ω Foreground ω	0.60394 0.03379 0.03379	0.02154 1 1	0.36162 0.03379 1	0.0129 1 1
COX3	−14,342.36051 (64)	−14,342.36051 (65)	0(1)	Proportion Background ω Foreground ω	0.7732 0.03566 0.03566	0.05583 1 1	0.15946 0.03566 1	0.01151 1 1
CYTB	−23,569.97597 (64)	−23,568.82145 (65)	2.30904 (0.128)	Proportion Background ω Foreground ω	0.6602 0.05486 0.05486	0.12651 1 1	0.17899 0.05486 1.99219	0.0343 1 1.99219
ND1	−21,178.57394 (64)	−21,178.44627 (65)	0.25534 (0.613)	Proportion Background ω Foreground ω	0.7132 0.06267 0.06267	0.16247 1 1	0.10126 0.06267 1.3493	0.02307 1 1.3493
ND2	−27,990.92862 (64)	−27,990.92862 (65)	0(1)	Proportion Background ω Foreground ω	0.61005 0.15035 0.15035	0.38995 1 1	0 0.15035 1	0 1 1
ND3	−8436.363774 (64)	−8436.363774 (65)	0(1)	Proportion Background ω Foreground ω	0.51587 0.06222 0.06222	0.48413 1 1	0 0.06222 2.98105	0 1 2.98105
ND4	−33,740.52873 (64)	−33,737.52529 (65)	6.00689 (0.14)	Proportion Background ω Foreground ω	0.51219 0.10263 0.10263	0.35569 1 1	0.07797 0.10263 54.54094	0.05415 1 54.54094
ND4L	−7938.586789 (64)	−7938.586789 (65)	0(1)	Proportion Background ω Foreground ω	0.51716 0.11906 0.11906	0.12794 1 1	0.28452 0.11906 1	0.07039 1 1
ND5	−43,443.13895 (64)	−43,439.61876 (65)	7.040374 (0.007)	Proportion Background ω Foreground ω	0.48923 0.09697 0.09697	0.31608 1 1	0.11827 0.09697 80.31	0.07641 1 80.31
ND6	−13,066.49994 (64)	−13,069.9364 (65)	6.872916 (0.008)	Proportion Background ω Foreground ω	0.42345 0.13626 0.13626	0.57655 1 1	0 0.13626 18.70366	0 1 18.70366

Table 6. Parameter Estimates and Positively Selected Sites Identified Using the BEB Method for the Site Models (Model 8).

Gene	Estimates of Parameters	Positively Selected Sites	Pr (w > 1)	Post Mean +− SE for w
ND4L	p0 = 0.98871 (p1 = 0.01129) *p* = 0.92443 q = 15.49543 w = 1.00000	-	-	-
ND5	p0 = 0.99558 (p1 = 0.00442) *p* = 0.56877 q = 9.41966 w = 1.51283	190 - 469 F 487 I 491 -	0.556 0.577 0.694 0.656	2.865 ± 3.120 2.806 ± 2.970 3.343 ± 3.087 3.245 ± 3.161

Table 7. Positively Selected Sites Identified Using the BEB Method for the Branch-site Model.

Gene	Positively Selected Site (BEB)
ND4	12 A (0.718), 76 S (0.632), 94 A (0.669), 142 A (0.794), 175 S (0.657), 179 C (0.591), 208 A (0.888), 252 T (0.686), 255 T (0.525), 275 A (0.635), 289 S (0.584), 296 T (0.555), 321 V (0.885), 324 S (0.648), 345 A (0.607), 362 G (0.683), 372 A (0.774), 386 S (0.737), 389 C (0.636), 401 V (0.586), 421 S (0.696), 442 S (0.630), 465 L (0.601)
ND5	16 S (0.506), 21 L (0.633), 23 M (0.521), 65 W (0.926), 79 G (0.649), 83 C (0.790), 87 S (0.833), 101 V (0.807), 118 L (0.917), 149 S (0.677), 151 S (0.792), 158 A (0.778), 173 A (0.804), 181 H (0.787), 189 G (0.956), 209 A (0.759), 219 A (0.517), 251 V (0.554), 266 T (0.792), 275 A (0.875), 286 A (0.675), 330 T (0.769), 338 S (0.701), 347 W (0.826), 349 G (0.674), 354 Y (0.726), 358 W (0.727), 363 A (0.848), 369 M (0.928), 382 M (0.792), 388 H (0.714), 393 V (0.887), 419 T (0.877), 430 Q (0.600), 432 G (0.842), 433 S (0.908), 435 S (0.790), 437 A (0.535), 452 M (0.793), 463 L (0.534), 467 V (0.849), 519 T (0.856), 520 Q (0.516), 526 F (0.781), 537 L (0.610), 547 C (0.737), 551 C (0.889), 561 A (0.749), 576 V (0.913), 584 F (0.841), 586 T (0.529)

4. Conclusions

This study presents the first complete mitochondrial genome of the Korean endemic polychaete *Leiochrides yokjidoensis*, a species belonging to the taxonomically challenging family Capitellidae. Our phylogenomic analysis, utilizing 13 mitochondrial PCGs from 30 species, established the systematic position of *Leiochrides* for the first time. Unexpectedly, *Leiochrides* formed a sister group with clade comprising *Mediomastus*, *Barantolla*, *Heteromastus*, and *Notomastus hemipodus*, forming a distinct clade characterized by long branch lengths and unique gene rearrangements.

Our findings revealed a dynamic pattern of mitochondrial genome evolution within Capitellidae, linking evolutionary rates with genomic stability. We identified three distinct evolutionary modes: (1) a Conserved Group (including *Heteromastus* and *Notomastus hemipodus*) with stable gene orders; (2) a Hyper-variable Group (including *Notodasus*, other *Notomastus* species) showing extreme structural instability; and (3) a Divergent Group (*Leiochrides* and *Capitella*) exhibiting rapid evolution and unique gene orders. These results confirm the polyphyly of *Notomastus* and demonstrate that *Leiochrides* represents a distinct evolutionary lineage, phylogenetically distinct from the polyphyletic *Notomastus* complex, despite morphological similarities. Furthermore, the apparent similarity to *Capitella*, characterized by long branch lengths and positive selection signatures, suggests that *Leiochrides* may share a similar trajectory of rapid evolutionary adaptation to environmental pressures, akin to the opportunistic nature of *Capitella*. Additionally, the detection of positive selection in *ND4* and *ND5* genes suggests that *L. yokjidoensis* has likely undergone adaptive evolution to meet the metabolic demands of its specific subtidal benthic habitat.

By providing the first genomic reference for a formally identified *Leiochrides* species, this study serves as a foundational genomic cornerstone. It offers a high-confidence anchor point for resolving the "morphological mosaic" of Capitellidae and paves the way for future studies to clarify the complex systematics of this family using a phylogenomic approach.

Author Contributions: Conceptualization, S.-i.E. and M.-K.J.; methodology, D.-H.K., J.Y., J.K. and H.O.; formal analysis, D.-H.K., J.Y., J.K., H.K. and H.O.; investigation, D.-H.K., J.Y. and H.O.; resources, S.-i.E. and M.-K.J.; data curation, S.-i.E.; writing—original draft preparation, D.-H.K. and J.Y.; writing—review and editing, S.-i.E. and M.-K.J.; visualization, D.-H.K. and J.Y.; supervision, S.-i.E. and M.-K.J.; project administration, S.-i.E. and M.-K.J.; funding acquisition, S.-i.E. and M.-K.J. All authors have read and agreed to the published version of the manuscript.

Funding: This research was supported by the National Marine Biodiversity Institute of Korea (MABIK) through the "Management of Marine Fishery Bio-resources Center" program (2025), Korea Institute of Marine Science & Technology Promotion (RS-2025-02215227) funded by the Ministry of Oceans and Fisheries, and Chung-Ang University Graduate Research Scholarship in 2025.

Institutional Review Board Statement: The experimental protocols received approval from the Institutional Animal Care and Use Committee (IACUC) at Chonnam National University (CNU IACUC-YS-2023–9).

Data Availability Statement: The raw next-generation sequencing data generated in this study have been deposited in the NCBI Sequence Read Archive (SRA) under accession number SRR36107181. The complete mitochondrial genome sequence of *Leiochrides yokjidoensis* assembled in this work is accessible via the NCBI GenBank database under accession number PX614612.

Conflicts of Interest: The authors declare that they have no competing interests.

References

1. Weigert, A.; Bleidorn, C. Current status of annelid phylogeny. *Org. Divers. Evol.* **2016**, *16*, 345–362. [CrossRef]
2. Grube, A.E. Noch ein Wort über die Capitellen und ihre Stelle im Systeme der Anneliden. *Arch. Für Naturgeschichte* **1862**, *28*, 366–378.

3. Read, G.; Fauchald, K. (Eds.) World Polychaeta Database. Capitellidae Grube, 1862. World Register of Marine Species. 2025. Available online: https://www.marinespecies.org/aphia.php?p=taxdetails&id=921 (accessed on 8 November 2025).
4. Fauchald, K.; Jumars, P.A. The diet of worms: A study of polychaete feeding guilds. *Oceanogr. Mar. Biol. Annu. Rev.* **1979**, *17*, 193–284. [CrossRef]
5. Kristensen, E.; Kostka, J. Macrofaunal burrows and irrigation in marine sediment: Microbiological and biogeochemical interactions. *Interact. Between Macro-Microorg. Mar. Sediments* **2005**, *60*, 125–157.
6. Bannister, R.J.; Valdemarsen, T.; Hansen, P.K.; Holmer, M.; Ervik, A. Changes in benthic sediment conditions under an Atlantic salmon farm at a deep, well-flushed coastal site. *Aquac. Environ. Interact.* **2014**, *5*, 29–47. [CrossRef]
7. Blake, J.A.; Hilbig, B.; Scott, P.H. *Taxonomic Atlas of the Benthic Fauna of the Santa Maria Basin and Western Santa Barbara Channel: Vol. 7, The Annelida Part 4*; Science Applications International Corporation: Reston, VA, USA; U.S. Department of the Interior Minerals Management Service: Santa Maria, CA, USA, 1996.
8. Tomioka, S.; Kakui, K.; Kajihara, H. Molecular Phylogeny of the Family Capitellidae (Annelida). *Zool. Sci.* **2018**, *35*, 436–445. [CrossRef]
9. Purschke, G.; Böggemann, M.; Westheide, W. *Handbook of Zoology. Annelida. Volume 2 Pleistoannelida, Sedentaria II.*; Walter de Gruyter GmbH & Co KG: Berlin, Germany, 2020.
10. Rouse, G.; Pleijel, F.; Tilic, E. *Annelida*; Oxford University Press: Oxford, UK, 2022; p. 432.
11. Glasby, C.; Biriukova, O.; Martin, P.; Dyne, G.; Utevsky, S.; Wilson, R. Annelida–diagnoses, descriptions and keys to family-level taxa. *ARPHA Prepr.* **2024**, *5*, e137961.
12. Augener, H. Polychaeta II: Sedentaria. In *Die Fauna Südwest-Australiens. Ergebnisse der Hamburger Südwest-Australischen Forschungsreise 1905*; Michaelsen, W., Hartmeyer, R., Eds.; Gustav Fischer: Jena, Germany, 1914; Volume 5, pp. 1–72.
13. Jeong, M.K.; Wi, J.H.; Suh, H.L. A new species of *Leiochrides* from the Korean subtidal waters with notes on the taxonomic status of the genus Pseudomastus (Annelida, Capitellidae). *Zookeys* **2017**, *685*, 91–103. [CrossRef] [PubMed]
14. Jeong, M.K.; Soh, H.Y.; Suh, H.L. Three new species of *Heteromastus* (Annelida, Capitellidae) from Korean waters, with genetic evidence based on two gene markers. *Zookeys* **2019**, *869*, 1–18. [CrossRef] [PubMed]
15. Jeong, M.K.; Soh, H.Y.; Wi, J.H.; Suh, H.L. A new *Notomastus* (Annelida, Capitellidae) species from Korean waters, with genetic comparison based on three gene markers. *Zookeys* **2018**, *754*, 141–155. [CrossRef]
16. Jeong, M.-K.; Soh, H.Y. *Dasybranchus geojedoensis* sp. nov. (Annelida: Capitellidae), A New Capitellid Species from Southern Korea. *Diversity* **2020**, *12*, 290. [CrossRef]
17. Hartman, O. *Submarine Canyons of Southern California. Part III. Systematics Polychaetes*; University of Southern California Press: Los Angeles, CA, USA, 1963; p. 96.
18. Hartman, O. Polychaetous annelids of the Indian Ocean including an account of species collected by members of the International Indian Ocean Expeditions, 1963–1964 and a catalogue and bibliography of the species from India. *J. Mar. Biol. Assoc. India* **1974**, *16*, 191–252.
19. Green, K. Capitellidae (Polychaeta) from the Andaman Sea. *Phuket Mar. Biol. Cent. Spec. Publ.* **2002**, *24*, 249–343.
20. Blake, J. Chapter 4. Family Capitellidae Grube, 1862. In *Taxonomic Atlas of the Santa Maria Basin and Western Santa Barbara Channel. Vol. 7. Annelida Part 4. Polychaeta: Flabelligeridae to Sternaspidae*; Blake, J.A., Hilbig, B., Scott, P.V., Eds.; Santa Barbara Museum of Natural History: Santa Barbara, CA, USA, 2000; pp. 47–96.
21. Capaccioni-Azzati, R.; Martín, D. *Pseudomastus deltaicus*, gen. et sp. n. (Polychaeta: Capitellidae) from a shallow-water bay in the north-western Mediterranean Sea. *Zool. Scr.* **1992**, *21*, 247–250. [CrossRef]
22. Lin, J.; García-Garza, M.; Lyu, M.; Wang, J. A new species of *Notomastus* (Annelida, Capitellidae) from southern China, with remarks on its morphology and distribution. *ZooKeys* **2020**, *946*, 1–16. [CrossRef]
23. Hernandez-Alcantara, P.; Solis-Weiss, V. Capitellids (Polychaeta: Capitellidae) from the continental shelf of the Gulf of California, Mexico, with the description of a new species, *Notomastus angelicae*. *Proc. Biol. Soc. Wash.* **1998**, *111*, 708–719.
24. Hernández-Alcántara, P.; Solís-Weiss, V.; García-Garza, M.E. A new species of *Decamastus* Hartman, 1963 (Polychaeta: Capitellidae) from the Gulf of California, with remarks on its habitat. *Mar. Biodivers.* **2019**, *49*, 1123–1130. [CrossRef]
25. Lin, J.; Garcia-Garza, M.E.; Wang, J. First record of the genus *Leiocapitella* (Annelida: Capitellidae) from China with description of a new species. *Zootaxa* **2019**, *4604*, 191–196. [CrossRef] [PubMed]
26. Da Silva, C.F.; Amaral, A.C.Z. Redescription of *Leiocapitella atlantica* Hartman, 1965 and description of a new species from the Southeast Brazil (Annelida, Capitellidae). *Zootaxa* **2020**, *4767*, 518–530. [CrossRef] [PubMed]
27. Da Silva, C.F.; Amaral, A.C.Z. *Scyphoproctus* Gravier, 1904 (Annelida, Capitellidae): Description of three new species and relocation of *Heteromastides* Augener, 1914 in *Scyphoproctus*. *Zootaxa* **2019**, *4560*, 95–120. [CrossRef] [PubMed]
28. Su, X.; Yang, D.; Wu, X.; Sun, Y.; Qiu, J.-W.; Zhang, Y. Substantial mitochondrial gene order rearrangements and differential evolution rates within the family Capitellidae (Annelida). *Zoosystematics Evol.* **2025**, *101*, 955–967. [CrossRef]
29. Krueger, F. *Trim Galore!: A Wrapper Around Cutadapt and FastQC to Consistently Apply Adapter and Quality Trimming to FastQ Files, with Extra Functionality for RRBS Data*; Babraham Institute: Cambridge, UK, 2015.

30. Meng, G.; Li, Y.; Yang, C.; Liu, S. MitoZ: A toolkit for animal mitochondrial genome assembly, annotation and visualization. *Nucleic Acids Res.* **2019**, *47*, e63. [CrossRef] [PubMed]
31. Donath, A.; Jühling, F.; Al-Arab, M.; Bernhart, S.H.; Reinhardt, F.; Stadler, P.F.; Middendorf, M.; Bernt, M. Improved annotation of protein-coding genes boundaries in metazoan mitochondrial genomes. *Nucleic Acids Res.* **2019**, *47*, 10543–10552. [CrossRef]
32. Laslett, D.; Canbäck, B. ARWEN: A program to detect tRNA genes in metazoan mitochondrial nucleotide sequences. *Bioinformatics* **2008**, *24*, 172–175. [CrossRef] [PubMed]
33. Krzywinski, M.; Schein, J.; Birol, I.; Connors, J.; Gascoyne, R.; Horsman, D.; Jones, S.J.; Marra, M.A. Circos: An infor-mation aesthetic for comparative genomics. *Genome Res.* **2009**, *19*, 1639–1645. [CrossRef]
34. Jeon, M.S.; Jeong, D.M.; Doh, H.; Kang, H.A.; Jung, H.; Eyun, S. A practical comparison of the next-generation sequencing platform and assemblers using yeast genome. *Life Sci. Alliance* **2023**, *64*, e202201744. [CrossRef]
35. Choi, H.; Nam, J.; Yang, S.; Eyun, S. Highly contiguous genome assembly and gene annotation of the short-finned eel (*Anguillabicolor pacifica*). *Sci. Data* **2024**, *11*, 952. [CrossRef]
36. Katoh, K.; Standley, D.M. MAFFT multiple sequence alignment software version 7: Improvements in performance and usability. *Mol. Biol. Evol.* **2013**, *30*, 772–780. [CrossRef] [PubMed]
37. Aylward, F. *Introduction to Calculating dN/dS Ratios with Codeml V. 2. 2018*; Virginia Tech: Blacksburg, VI, USA, 2018.
38. Lanfear, R.; Frandsen, P.B.; Wright, A.M.; Senfeld, T.; Calcott, B. PartitionFinder 2: New methods for selecting partitioned models of evolution for molecular and morphological phylogenetic analyses. *Mol. Biol. Evol.* **2017**, *34*, 772–773. [CrossRef]
39. Kozlov, A.M.; Darriba, D.; Flouri, T.; Morel, B.; Stamatakis, A. RAxML-NG: A fast, scalable and user-friendly tool for maximum likelihood phylogenetic inference. *Bioinformatics* **2019**, *35*, 4453–4455. [CrossRef]
40. Huelsenbeck, J.P.; Ronquist, F. MRBAYES: Bayesian inference of phylogenetic trees. *Bioinformatics* **2001**, *17*, 754–755. [CrossRef]
41. Schneider, S.; Roessli, D.; Excoffier, L. Arlequin: A software for population genetics data analysis. *User Man. Ver* **2000**, *2*, 2496–2497.
42. Yang, Z. PAML 4: Phylogenetic analysis by maximum likelihood. *Mol. Biol. Evol.* **2007**, *24*, 1586–1591. [CrossRef] [PubMed]
43. Choi, H.; Gwon, Y.; An, Y.K.; Eyun, S. Positive Selection of Mitochondrial cytochrome b Gene in the Marine Bivalve *Keenocardium buelowi* (Bivalvia, Cardiidae). *Animals* **2024**, *14*, 2812. [CrossRef]
44. Kim, S.L.; Choi, H.; Eyun, S.; Kim, D.; Yu, O.H. A new Branchipolynoe (Aphroditiformia: Polynoidae) scale worm from the Onnuri Deep-sea hydrothermal vent field, northern Central Indian Ridge. *Zool. Stud.* **2022**, *61*, e21.
45. Kobayashi, G.; Itoh, H.; Nakajima, N. First mitochondrial genomes of Capitellidae and Opheliidae (Annelida) and their phylogenetic placement. *Mitochondrial DNA Part B* **2022**, *7*, 577–579. [CrossRef] [PubMed]
46. Acharya-Patel, N.; Cram, K.; Groenwold, E.T.; Lee, H.; Keller, A.G.; Bomback, B.; Lyons, S.; Warren, R.L.; Coombe, L.; Lowe, C.J.; et al. Monitoring marine pollution effects through targeted environmental DNA (eDNA) testing in the Pacific northwest. *Mar. Pollut. Bull.* **2025**, *216*, 118036. [CrossRef]
47. Kobayashi, G.; Itoh, H.; Nakajima, N. First mitochondrial genome of a lugworm (Annelida: Arenicolidae) and its phylogenetic position. *J. Mar. Biol. Assoc. U. K.* **2022**, *102*, 635–644. [CrossRef]
48. Jennings, R.M.; Halanych, K.M. Mitochondrial genomes of *Clymenella torquata* (Maldanidae) and *Riftia pachyptila* (Siboglinidae): Evidence for conserved gene order in Annelida. *Mol. Biol. Evol.* **2005**, *22*, 210–222. [CrossRef] [PubMed]
49. Bleidorn, C.; Podsiadlowski, L.; Bartolomaeus, T. The complete mitochondrial genome of the orbiniid polychaete *Orbinia latreillii* (Annelida, Orbiniidae)–A novel gene order for Annelida and implications for annelid phylogeny. *Gene* **2006**, *370*, 96–103. [CrossRef]
50. Huč, S.; Hiley, A.S.; McCowin, M.F.; Rouse, G.W. A mitogenome-based phylogeny of Pilargidae (Phyllodocida, Polychaeta, Annelida) and evaluation of the position of Antonbruunia. *Diversity* **2024**, *16*, 134. [CrossRef]
51. Kim, D.-H.; Ryu, S.J.; Kim, J.R.; Eyun, S.; Jeong, M.-K. The Complete Mitochondrial Genome of the Korean Endemic Polychaete *Phyllodoce koreana* (Lee & Jae, 1985) from Jindong Bay, Korea, with Additional Morphological and Ecological Features. *J. Mar. Sci. Eng.* **2025**, *13*, 223. [CrossRef]
52. Choi, H.; Yu, O.; Eyun, S. Evolutionary insights into adaptation of hemocyanins from deep-sea hydrothermal vent shrimps. *Mar. Pollut. Bull.* **2025**, *215*, 117872. [CrossRef] [PubMed]